March 2004

Low-Temperature Fabrication of Oxide Composites for Solid-Oxide Fuel Cells

Hongpeng He
University of Pennsylvania

Yingyi Huang
University of Pennsylvania

Juleiga Regal
University of Pennsylvania

Marta Boaro
University of Pennsylvania

John M. Vohs
University of Pennsylvania, vohs@seas.upenn.edu

See next page for additional authors

Low-Temperature Fabrication of Oxide Composites for Solid-Oxide Fuel Cells

Abstract

Composites of yttria-stabilized zirconia (YSZ) with Sr-doped $LaCrO_3$ (LSC) and Sr-doped $LaMnO_3$ (LSM) were prepared by impregnation of a porous YSZ matrix with aqueous solutions of the appropriate metal salts, followed by sintering to various temperatures. XRD measurements showed that perovskite phases formed after sintering at 1073 K, a temperature well below that at which solid-state reactions with YSZ occur. The conductivities of the LSC–YSZ and LSM–YSZ composites prepared in this way were maximized at a sintering temperature of 1373 K for LSC–YSZ and 1523 K for LSM–YSZ, although reasonable conductivities were achieved at much lower temperatures. The conductivities of the two composites increased much more rapidly with the content of the conductive oxide than has been found with conventional composites formed by mixing and sintering the oxide powders. The implications for using this approach to develop novel electrodes for SOFC applications are discussed.

Author(s)

Hongpeng He, Yingyi Huang, Juleiga Regal, Marta Boaro, John M. Vohs, and Raymond J. Gorte

journal

J. Am. Ceram. Soc., 87 [3] 331–36 (2004)

Low-Temperature Fabrication of Oxide Composites for Solid-Oxide Fuel Cells

Hongpeng He, Yingyi Huang, Juleiga Regal, Marta Boaro, John M. Vohs, and Raymond J. Gorte*

Department of Chemical Engineering, University of Pennsylvania, Philadelphia, Pennsylvania 19104

Composites of yttria-stabilized zirconia (YSZ) with Sr-doped $LaCrO_3$ (LSC) and Sr-doped $LaMnO_3$ (LSM) were prepared by impregnation of a porous YSZ matrix with aqueous solutions of the appropriate metal salts, followed by sintering to various temperatures. XRD measurements showed that perovskite phases formed after sintering at 1073 K, a temperature well below that at which solid-state reactions with YSZ occur. The conductivities of the LSC–YSZ and LSM–YSZ composites prepared in this way were maximized at a sintering temperature of 1373 K for LSC–YSZ and 1523 K for LSM–YSZ, although reasonable conductivities were achieved at much lower temperatures. The conductivities of the two composites increased much more rapidly with the content of the conductive oxide than has been found with conventional composites formed by mixing and sintering the oxide powders. The implications for using this approach to develop novel electrodes for SOFC applications are discussed.

I. Introduction

THE electrodes in solid-oxide fuel cells (SOFCs) are typically made from a composite of an electronically conductive material with an electrolyte oxide. For example, with electrolytes made from yttria-stabilized zirconia (YSZ), the conventional anode is a Ni–YSZ ceramic–metallic (cermet) composite.[1–3] In addition to maintaining porosity in the anode and providing a coefficient of thermal expansion (CTE) match with the electrolyte, the YSZ in the cermet extends the region into which ions can migrate, which increases the length of the three-phase boundary (TPB). A material commonly used for SOFC cathodes is a composite of YSZ with Sr-doped $LaMnO_3$ (LSM).[4–8] Just as with the nickel cermets, YSZ in the LSM–YSZ composite provides a path for ion migration to extend the TPB region within the cathode.[9]

Great care must be taken in the preparation of oxide composites, such as LSM and YSZ, so as to avoid solid-state reactions that lead to insulating phases.[10–13] In general, the two oxide phases are fabricated separately, physically mixed, and then heated.[14,15] The temperature must be high enough to sinter the ion-conducting component in the electrode to the electrolyte,[9] but this temperature must be low enough to prevent solid-state reactions between the two oxide phases. In the case of LSM–YSZ composites, sintering above 1523 K is recognized as leading to $La_2Zr_2O_7$.[16–18] Because YSZ powders do not sinter to a significant extent below ~1373 K, the conditions for achieving optimal electrode properties from oxide composites are rather limited. Indeed, it is not possible to prepare some oxide composites because the sintering temperature for YSZ is higher than the temperature at which solid-state reactions occur between the two oxides.

In our laboratory, we have developed a different approach to the fabrication of electrode composites to prepare copper–cermet anodes for SOFCs that convert hydrocarbons directly, without first reforming the fuel to H_2 and CO.[19–23] Because Cu_2O and CuO melt at 1508 and 1599 K, respectively, conventional methods for preparing Cu–YSZ cermets are not effective. Our approach has been to synthesize a highly porous YSZ that has been heated to high temperatures together with the electrolyte and then to add the copper by impregnation of the porous YSZ with soluble salts of copper. The metallic phase of the copper can be obtained in low-temperature sintering and reduction procedures, avoiding any solid-state reactions that can occur between CuO_x and YSZ.

In this article, the results of a study in which a similar approach has been used to prepare composites of YSZ with LSM and with Sr-doped $LaCrO_3$ (LSC) are reported. LSC has been suggested for use in ceramic anodes, because it is stable and electronically conductive under reducing environments.[24–27] LSC–YSZ composites can potentially combine the electronic properties of the LSC with the ionic conductivity of the YSZ in the same way as LSM–YSZ composites. The results indicate that this synthesis method prevents the formation of undesirable mixed oxides and forms composites with a structure different from that prepared by conventional methods, which suggests that the method is worth further investigation for the synthesis of electrode materials.

II. Experimental Procedure

The LSC–YSZ and LSM–YSZ composites were each prepared by two methods: method A involved conventional, physical mixing of the oxide powders, while method B involved impregnation of a porous YSZ matrix with metal salts. For method A, the YSZ (TZ, 84.8% Y_2O_3, 0.2 μm, Tosoh Corp., Tokyo, Japan) and LSM ($La_{0.8}Sr_{0.2}MnO_3$, Praxair Surface Technologies, Woodinville, WA) were used as-received. LSC ($La_{0.7}Sr_{0.3}CrO_{3-\delta}$) was synthesized from the nitrate salts of $La(NO_3)_3 \cdot 6H_2O$ (ACS 99.9%, Alfa Aesar, Ward Hill, MA), $Sr(NO_3)_2$ (ACS 99.0%, Alfa Aesar), and $Cr(NO_3)_3 \cdot 9H_2O$ (ACS 98.5%, Alfa Aesar). After the salts were dissolved in distilled water, the mixture was dried and calcined at 1073 K in air overnight. This powder was ground in a mortar and pestle in the presence of isopropyl alcohol, sintered in air at 1673 K for 4 h, and then ground again. The resulting powder was shown to have the correct perovskite structure using X-ray diffractometry (XRD). Finally, the LSM–YSZ and LSC–YSZ composites were prepared by physically mixing the oxide powders, uniaxially pressing them into wafers, and sintering the wafers to various temperatures.

To prepare composites by impregnation, method B, we first prepared a porous YSZ matrix using procedures that have been described elsewhere.[22] The YSZ powder was mixed with distilled water, a dispersant (Duramax 3005, Rohm & Haas, Woburn, MA), binders (HA12 and B1000, Rohm & Haas), and pore formers (graphite and poly(methyl methacrylate)). This slurry was either cast into tapes that would result in porous ceramic wafers, 600 μm

R. Steinbrech—contributing editor

Manuscript No. 186414. Received November 11, 2002; approved October 3, 2003.
Supported by the Office of Naval Research.
*Member, American Ceramic Society.

thick, or formed into rectangular pieces, 2 mm × 2 mm × 10 mm. The YSZ wafers and rectangular pieces were sintered to 1823 K, which resulted in a porosity of 60%, as shown by the weight change of the sample after water immersion.[22] Either LSM or LSC was then added to the porous YSZ through impregnation of the YSZ with an aqueous solution containing the appropriate concentrations of the nitrate salts of lanthanum, strontium, and either chromium or manganese ($Mn(NO_3)_2 \cdot xH_2O$, ACS 99.98%, Alfa Aesar).

Electrical conductivities were measured using the standard four-probe direct-current method. The samples were placed in a holder, and external platinum foils were attached to both ends. Current from an electrochemical interface (Model 1286, Solartron, Houston, TX) was passed through the samples while monitoring the voltage across the samples using a multimeter (Model 72–410A, Tenma). The conductivities were typically measured either in air or in humidified H_2. For the LSM–YSZ composites, most of the samples were prepared from the rectangular pieces, while the results for the LSC–YSZ composites were obtained from the 600 μm wafers. The phase and microstructure of selected samples were also investigated using XRD and scanning electron microscopy (SEM; Model JSM-6300LV, JEOL, Tokyo, Japan).

III. Results

Before discussing the structural and conductivity data for the LSC–YSZ and LSM–YSZ composites, it is important to establish that the mixed oxides prepared using method B have the conducting oxide within the porous YSZ matrix. In Fig. 1, the porosities of the mixed oxides are shown for a series of materials with increasing amounts of LSM or LSC. The LSC–YSZ composites in Fig. 1 were heated to 1373 K and the LSM–YSZ composites were heated to 1523 K. For this data, the porosity of the composites was determined from the mass change after water immersion,[22] while the volume of either LSM or LSC was calculated from the mass of oxide that was added to the porous YSZ, using the bulk densities for LSM and LSC. The line in Fig. 1 is the expected change in porosity of the composite assuming the second oxide fills the pores. The fact that the experimental porosities agree with the calculated changes demonstrates that the second oxide remains in the pore structure following the heat treatments. If the LSM or LSC had left the YSZ pore structure, one would expect the porosities to change more slowly with the addition of the second oxide.

(1) LSC–YSZ Composites

Figures 2 and 3 provide SEM results for the LSC–YSZ composites made using the two methods. Figure 2 shows the mixed powder, with 48 vol% LSC, after it was sintered to 1373 K. (The volume percent is calculated based on the entire volume of the composite, including pores.) The material consists of relatively uniform particles, ~0.2 μm in diameter, with a porosity of ~25%. In this sample, the YSZ and LSC particles are the same size and

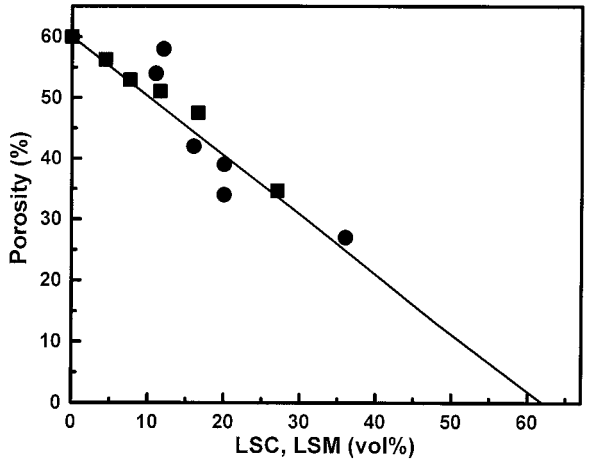

Fig. 1. Porosity of YSZ composites with LSM and LSC, prepared by impregnation ((—) expected result assuming the oxides exist in the YSZ pores, (●) LSC, and (■) LSM).

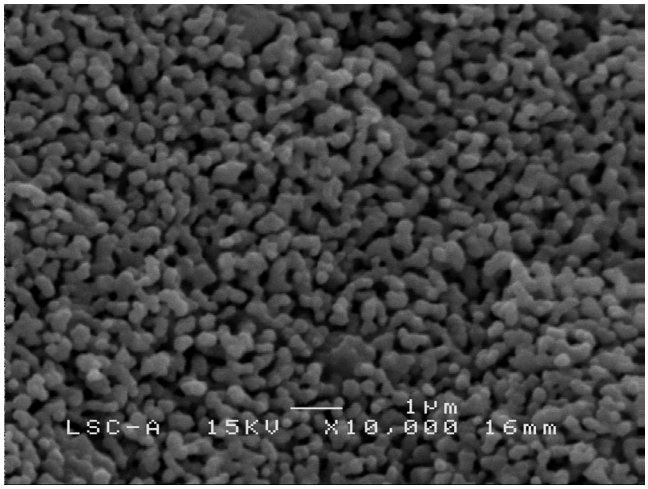

Fig. 2. SEM image of LSC–YSZ composite prepared by sintering of the mixed powders.

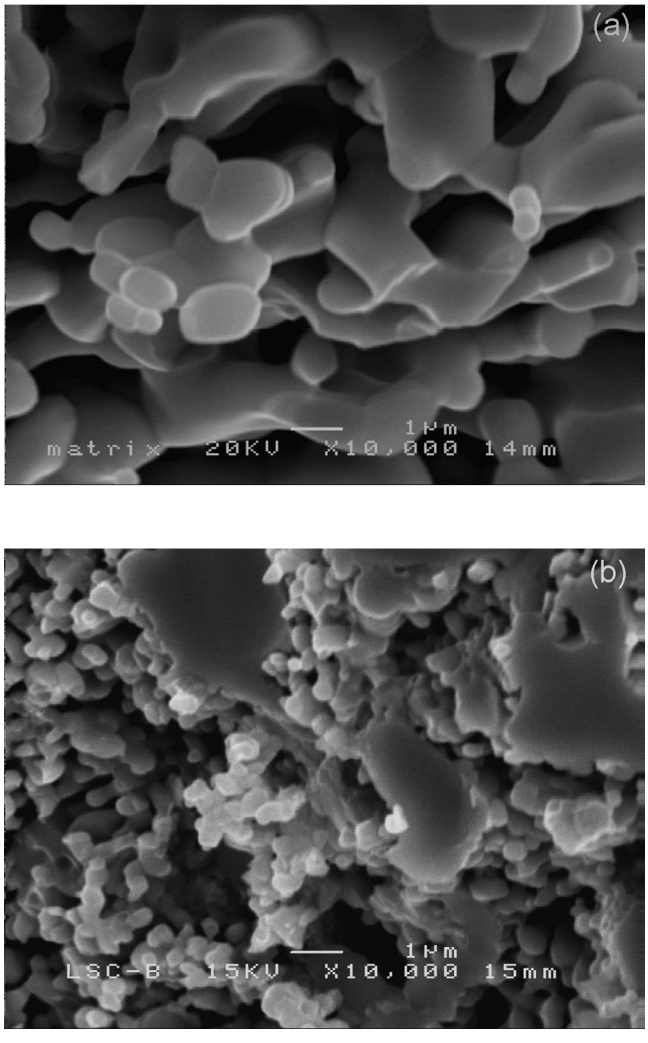

Fig. 3. SEM images of (a) the initial YSZ matrix and (b) the LSC–YSZ composite prepared by impregnation.

indistinguishable. Figure 3 shows the porous YSZ, before and after addition of LSC to a level of 40 vol% by impregnation of the porous YSZ with the lanthanum, strontium, and chromium salts. The porous, YSZ matrix (Fig. 3(a)) consists of smooth, relatively uniform pores, ~1–2 μm in size. After impregnation, 0.2 μm LSC particles are observed coating the YSZ walls, as shown in Fig. 3(b). Obviously, the structure and connectivity of the LSC are very different from the composite sample made using method B.

Figure 4 shows the XRD patterns following impregnation of the porous YSZ with the lanthanum, strontium, and chromium salts to a loading of 23 vol% LSC, after heating to increasingly higher temperatures. Peaks corresponding to the LSC perovskite phase (notably, those peaks at 41°, 46°, 58°, 68°, and 78° 2θ) become apparent beginning at ~1073 K. These peaks become sharper after sintering above 1373 K, but a new peak at 31°, due to $SrZrO_3$, appears at a sintering temperature of 1473 K. For temperatures below 1673 K, there are also several overlapping peaks in the region near 41° 2θ, which are probably associated with chromium compounds, such as CrO, $CrO_2(OH)_y$, and $Cr(OH)_y$.[28]

To determine the optimal sintering temperature for obtaining the maximum conductivity from the composites, we measured the conductivities of 25 wt% LSC composites prepared by both methods as a function of temperature, with the results shown in Fig. 5. For method B, this composition also corresponds to ~23 vol% LSC; however, the volume percent of LSC changed with sintering temperature for the sample made using method A, because the sample density changed (~22 vol%). The samples were heated in air for 2 h at the indicated temperatures before the temperature was decreased to 973 K, and the conductivities were measured in air and humidified (3 mol% H_2O) H_2. For the composite made using method B, the conductivity increased with

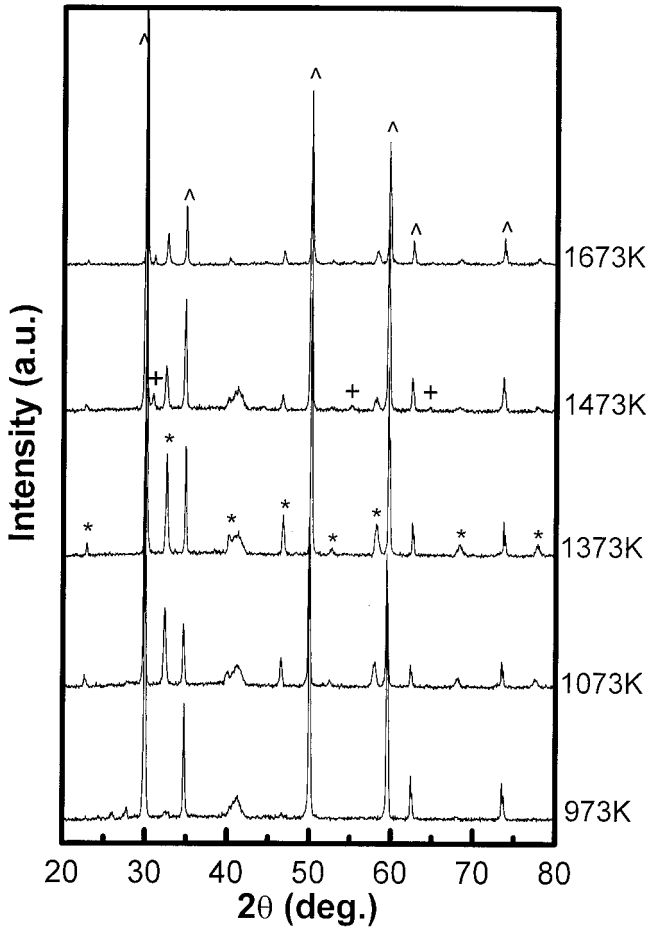

Fig. 4. XRD patterns of the LSC–YSZ composite, prepared by impregnation, following various sintering temperatures ((⋆) LSC, (/\) YSZ, and (+) $SrZrO_3$ phases).

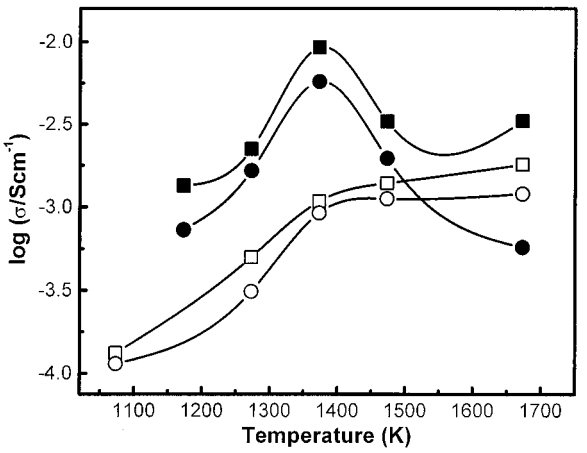

Fig. 5. Electrical conductivities at 973 K of LSC–YSZ composites as a function of sintering temperature. Data are shown for composites formed from mixed powders (□) in air and (○) in H_2 and by impregnation (■) in air and (●) in H_2.

temperature to a maximum value at 1373 K, then decreased following sintering to higher temperatures. This was consistent with higher conductivity caused by the formation of the LSC phase up to 1373 K. The conductivity decreased at higher temperatures because of the formation of secondary, insulating phases. The conductivity of the composite formed at the highest temperature was sensitive to the gas-phase composition, while the composite formed at the optimal temperature of 1373 K was not sensitive. Because LSC remained conductive over a wide range of oxygen partial pressure (P_{O_2}), the relatively high conductivity observed in air on the sample sintered to 1673K may not have been due to LSC.

For the 25 wt% LSC composite prepared using method A, the conductivity increased with increased temperature, up to 1673 K, and there was not much difference between the conductivities measured in air and in H_2. The reason for increased conductivity with sintering temperature was different in this case, because the conductive LSC phase already had been formed before it was mixed with YSZ. For this sample, increased temperature increased the density, which in turn improved the connectivity of the conductive phase. The rather small increase in conductivity that was observed between 1373 and 1673 K probably was due to counteracting effects, and the formation of secondary phases decreased the conductivity and densification increased the conductivity.

Figure 6 shows the effect of composition on the conductivity of the LSC–YSZ composites. All the samples were sintered to 1373 K for 2 h before their conductivities were measured in air and humidified H_2 at 973 K. The samples prepared using method B showed reasonably high conductivities at relatively low volume fractions of LSC. This was almost certainly due to the structure of the impregnated composites, in which the LSC coated the walls of the YSZ matrix.

For the samples prepared using method A, the conductivity was low until the volume fraction of LSC reached ~80%. The fact that such a high weight fraction of LSC was required, much higher than would be expected based on percolation concepts, was due to the low density of these powders after they were sintered at 1373 K. This is shown in Fig. 7. Here, the densities of the samples used for the data in Fig. 6 are plotted as a function of composition, along with a line that shows the theoretical density of a nonporous composite of LSC–YSZ. Obviously, the composites with <80 vol% LSC are highly porous.

(2) LSM–YSZ Composites

The structure of LSM–YSZ composites prepared by impregnation of the nitrate salts of lanthanum, strontium, and manganese

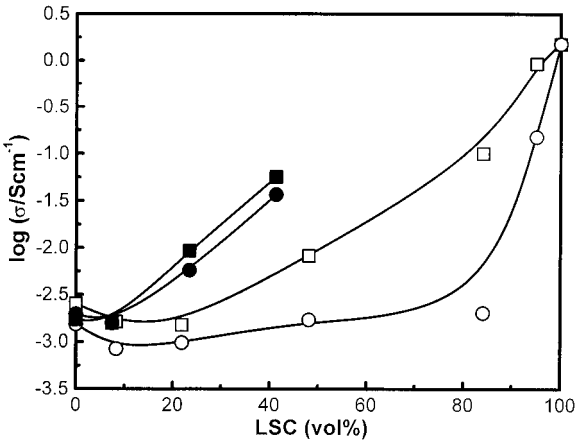

Fig. 6. Electrical conductivities at 973 K for LSC–YSZ composites as a function of composition. Data are shown for samples prepared from the mixed powders (□) in air and (○) in H_2 and by impregnation (■) in air and (●) in H_2.

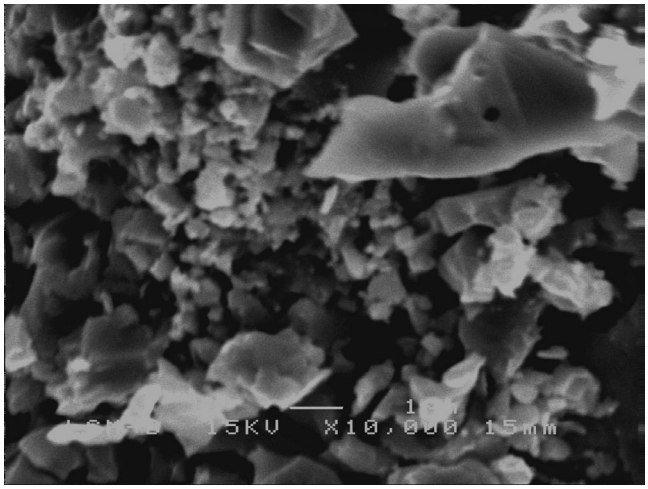

Fig. 8. SEM image of LSM–YSZ composite prepared by impregnation.

was very similar to that observed for the related LSC–YSZ composite. Figure 8 is a micrograph of a 28 vol% LSM–YSZ composite after it was sintered to 1523 K, prepared using a porous YSZ support similar to that shown in Fig. 3(b). Again, small LSM particles were observed coating the walls of the YSZ matrix. While we do not show micrographs of LSM–YSZ composites prepared using method A, we observed that the composites prepared by method A were essentially dense after heating to 1523 K, with porosities <3%.

Figure 9 shows the electrical conductivity at 973 K, in air, of a 28 vol% LSM–YSZ composite prepared using method B, as a function of sintering temperature. Similar to what occurred with the LSC–YSZ composites, the conductivity reached a maximum with sintering temperature. However, the maximum conductivity was now considerably higher and was achieved at ~1523 K. The absolute change in conductivity was relatively small in this case, and the conductivity of the composite was already quite high at 1073 K. The optimal temperature, 1523 K, was approximately the recommended temperature for sintering LSM–YSZ composites, prepared using traditional methods, for use as SOFC cathodes.[29]

To better understand the structures that resulted in this conductivity, XRD measurements were performed on a sample prepared by impregnation of porous YSZ to a loading that corresponded to 28 vol% LSM, after it was heated to various temperatures. These results are shown in Fig. 10. Peaks at 23°, 33°, 41°, 47°, and 58° 2θ, associated with the perovskite phase, appeared at 1073 K. Small peaks due to the $La_2Zr_2O_7$ phase (29°, 48°, and 57° 2θ) were observed at 1523 K, and these continued to grow with increased temperature. It seemed likely that the increase in conductivity of the sample in going from 1073 to 1523 K was due to increased crystallinity of the LSM phase with sintering; the decreased conductivity at higher temperatures was due to the formation of the insulating $La_2Zr_2O_7$ phase.

Figure 11 provides the conductivities of LSM–YSZ composites, prepared by both methods, as a function of LSM content. The samples prepared using method A were sintered to 1523 K for 2 h; conductivities were reported for impregnated samples that had been heated to either 1073 or 1523 K. Several interesting observations could be drawn from this data. First, unlike the LSC–YSZ composites, the LSM–YSZ composites prepared using the traditional, mixed-powder method were reasonably dense, with porosities <3%, and they exhibited high conductivities at reasonable LSM contents. Indeed, the conductivity of the composites prepared using physical mixing increased rapidly at an LSM concentration of ~28 vol%, which was the expected value for percolation in random media. Second, as we observed with the LSC–YSZ composites, the conductivities of the impregnated samples were much higher at the low LSM contents because of formation of particles on the porous, YSZ walls. Third, the conductivities of the LSM–YSZ composites formed using method B were already high after being sintered to only 1073 K. The obvious implication was

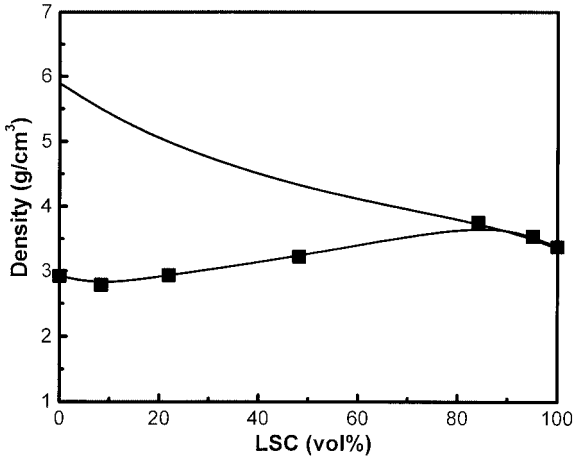

Fig. 7. Densities of LSC–YSZ composites prepared from the mixed powders after they were sintered at 1373 K. Data are plotted along with the calculated density assuming no porosity.

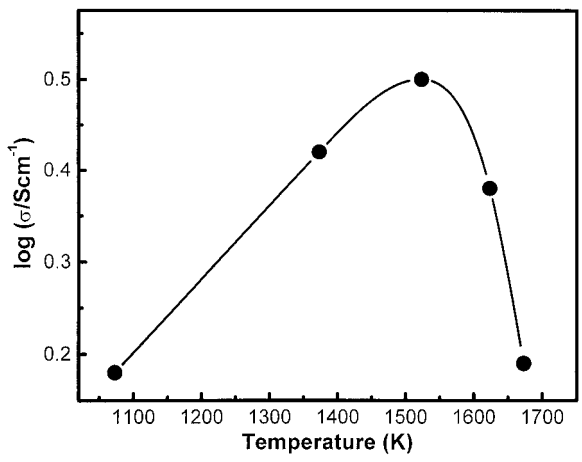

Fig. 9. Conductivity of the LSM–YSZ (28 vol% LSM) composite, prepared by impregnation, as a function of sintering temperature. Data were obtained at 973 K in air.

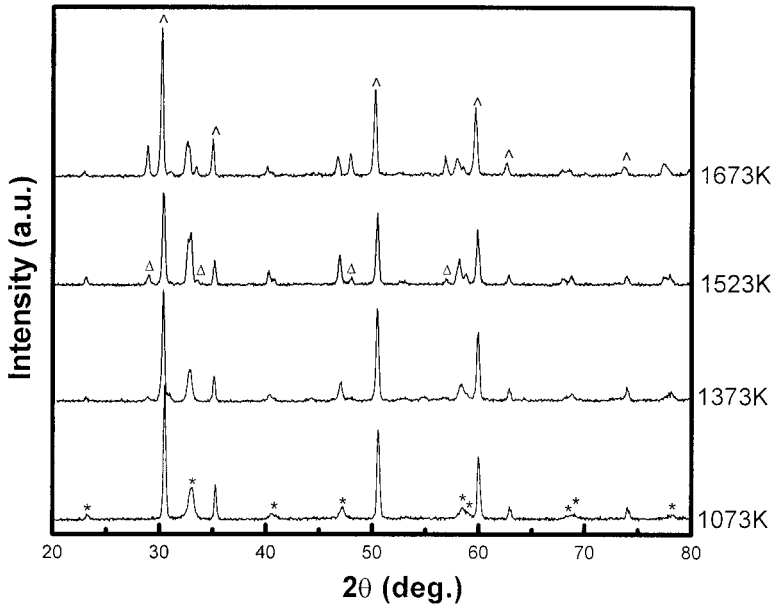

Fig. 10. XRD patterns of the LSM–YSZ composite, prepared by impregnation, as a function of sintering temperature ((⋆) LSM, (Δ) $La_2Zr_2O_7$, and (∧) YSZ phases).

that reasonable electronic properties could be obtained with very low processing temperatures.

IV. Discussion

Recent interest in decreasing the operating temperature of SOFCs has led to renewed investigations into alternative cathode materials. For example, Sr-doped $LaFeO_3$ (LSF) and Sr-doped $LaCoO_3$ (LSCo) exhibit superior performance as SOFC cathodes compared with LSM.[30–33] However, because these materials react with YSZ at temperatures lower than that necessary for synthesis of the cell, it is usually necessary to avoid contact between YSZ and either LSF or LSCo by incorporating an additional material in the cathode as a barrier.[32,33] Even without changing the material, the performance of LSM–YSZ composites can be significantly enhanced by tailoring the microstructure.[34] The formation of oxide composites by impregnation of the components of one oxide into a porous matrix of the second oxide presents interesting opportunities for the optimization of composition and microstructure in oxide composites and clearly deserves additional investigation.

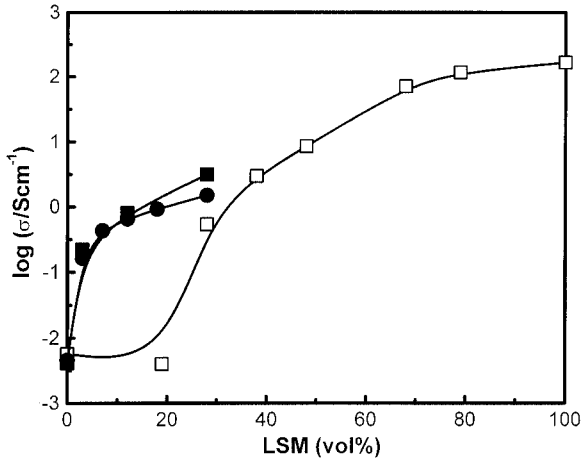

Fig. 11. Electrical conductivities at 973 K for LSM–YSZ composites as a function of composition. Data are shown for samples prepared from the (□) mixed powders and by impregnation followed by sintering to (■) 1523 or (●) 1073 K.

Regarding composition, the work in this article demonstrates that conductive, perovskite phases can be prepared for LSM and LSC below 1073 K. This temperature is low enough that solid-state reactions should not present problems. Because this temperature is similar to the operating temperature of an SOFC, it may not be necessary to have a separate sintering step to form the composite. Furthermore, the LSM and LSC phases are formed below 1073 K without the use of special precursors to promote mixing of the metal cations that make up the perovskite structures;[34] the salts used in this study have been chosen simply for their solubility and price. Finally, it is likely that the doped $LaFeO_3$ and $LaCoO_3$ phases can be formed by similar procedures.

Regarding microstructure, the synthesis of the second oxide phase within the preexisting YSZ matrix has several potential advantages. First, various sintering temperatures can be used in the preparation of the two oxide phases. With YSZ, high temperatures are advantageous for preparing an interconnected network in which ions can pass freely from the electrolyte to the YSZ within the electrode.[9] Obviously, this porous structure can be formed along with the dense electrolyte through the use of bilayers,[20] so that very good connectivity can be established between the electrolyte and electrode layers. Second, a wide range of pore sizes and porosities can be established in the YSZ through the use of various pore formers and YSZ particle sizes.[22,35,36] Therefore, it is relatively easy to control the microstructure of the YSZ phase.

Our results demonstrate that the materials made by impregnation cannot be modeled as random distributions of the oxide phases. Because the second phase tends to coat the walls of the YSZ matrix, high conductivities can be obtained at low volume fractions of the conductive oxide. Again, for applications in which it is necessary to limit the amount of conductive oxide that is used, this property can be advantageous.

Finally, the LSC–YSZ composite results demonstrate that it may be possible to form novel, composite oxides for anodes as well as cathodes. Ceramic anodes show great promise for SOFCs that convert hydrocarbons directly, without first reforming those hydrocarbons to syngas;[24–27,37] however, these oxides are often used in their pure form on electrolyte-supported cells. By impregnating conducting oxides into a porous matrix, it should be possible to make anode-supported cells with thin electrolytes, with enhanced three-phase boundaries caused by good connection between the electrolyte and electrode phases.

V. Conclusions

We have shown that it is possible to fabricate composite oxides of YSZ with LSM or LSC by impregnation of a porous YSZ matrix with solutions of the metal salts that are precursors to LSM or LSC. The LSM and LSC perovskite phases are formed at temperatures below 1073 K, a temperature low enough to avoid solid-state reactions with the YSZ. The structure of the LSM–YSZ and LSC–YSZ composites made by impregnation is shown to be very different from composites made by mixing the oxide phases, allowing reasonable electronic conductivities to be observed at relatively low concentrations of the conductive oxide. These composite oxides show promise for application as SOFC electrodes.

References

[1]J. V Herle, R. Ihringer, R. V. Cavieres, L. Constantin, and O. Bucheli, "Anode-Supported Solid-Oxide Fuel Cells with Screen-Printed Cathodes," *J. Eur. Ceram. Soc.*, **21** [10–11] 1855–59 (2001).

[2]Y. Li, Y. S. Xie, J. H. Gong, Y. F. Chen, and Z. T. Zhang, "Preparation of Ni/YSZ Materials for SOFC Anodes by Buffer-Solution Method," *Mater. Sci. Eng. B-Solid State Mater. Adv. Technol.*, **86** [2] 119–22 (2001).

[3]J. H. Lee, H. Moon, H. W. Lee, J. Kim, J. D. Kim, and K. H. Yoon, "Quantitative Analysis of Microstructure and Its Related Electrical Property of SOFC Anode, Ni–YSZ Cermet," *Solid State Ionics*, **148** [1–2] 15–26 (2002).

[4]J. W. Yan, Z. G. Lu, Y. Jiang, Y. L. Dong, C. Y. Yu, and W. Z. Li, "Fabrication and Testing of a Doped Lanthanum Gallate Electrolyte Thin-Film Solid-Oxide Fuel Cell," *J. Electrochem. Soc.*, **149** [9] A1132–A1135 (2002).

[5]J. H. Koh, Y. S. Yoo, J. W. Park, and H. C. Lim, "Carbon Deposition and Cell Performance of Ni-YSZ Anode Support SOFC with Methane Fuel," *Solid State Ionics*, **149** [3–4] 157–66 (2002).

[6]S. P. Jiang, J. G. Love, and Y. Ramprakash, "Electrode Behaviour at (La, Sr)MnO_3/Y_2O_3–ZrO_2 Interface by Electrochemical Impedance Spectroscopy," *J. Power Sources*, **110** [1] 201–208 (2002).

[7]A. Barbucci, R. Bozzo, G. Cerisola, and P. Costamagna, "Characterisation of Composite SOFC Cathodes Using Electrochemical Impedance Spectroscopy. Analysis of Pt/YSZ and LSM/YSZ Electrodes," *Electrochim. Acta*, **47** [13–14] 2183–88 (2002).

[8]N. T. Hart, N. P. Brandon, M. J. Day, and N. Lapena-Rey, "Functionally Graded Composite Cathodes for Solid-Oxide Fuel Cells," *J. Power Sources*, **106** [1–2] 42–50 (2002).

[9]D. Herbstritt, A. Weber, and E. Ivers-Tiffee, "Modelling and DC-Polarisation of a Three-Dimensional Electrode/Electrolyte Interface," *J. Eur. Ceram. Soc.*, **21** [10–11] 1813–16 (2001).

[11]L. Kindermann, D. Das, H. Nickel, K. Hilpert, C. C. Appel, and F. W. Poulson, "Chemical Compatibility of $(La_{0.6}Ca_{0.4})_xFe_{0.8}M_{0.2}O_3$ with Yttria-Stabilized Zirconia," *J. Electrochem. Soc.*, **144** [2] 717–20 (1997).

[12]H. Kamata, A. Hosaka, J. Mizusaki, and H. Tagawa, "Chemical Compatibility of Perovskite-Type Oxide $La_{0.7}Ca_{0.3}Cr_{1-y}Co_yO_3$ with Y_2O_3-Stabilized ZrO_2," *Mater. Res. Bull.*, **30** [6] 679–87 (1995).

[12]G. Stochniol, E. Syskakis, and A. Naoumidis, "Chemical Compatibility between Strontium-Doped Lanthanum Manganite and Yttria-Stabilized Zirconia," *J. Am. Ceram. Soc.*, **78** [4] 929–32 (1995).

[13]G. C. Kostogloudis, G. Tsiniarakis, and C. Ftikos, "Chemical Reactivity of Perovskite Oxide SOFC Cathodes and Yttria-Stabilized Zirconia," *Solid State Ionics*, **135** [1–4] 529–35 (2000).

[14]J. D. Kim, G. D. Kim, J. W. Moon, Y. I. Park, W. H. Lee, K. Kobayashi, M. Nagai, and C. E. Kim, "Characterization of LSM–YSZ Composite Electrode by AC Impedance Spectroscopy," *Solid State Ionics*, **143** [3–4] 379–89 (2001).

[15]J. H. Choi, J. H. Jang, and S. M. Oh, "Microstructure and Cathodic Performance of $La_{0.9}Sr_{0.1}MnO_3$/Yttria-Stabilized Zirconia Composite Electrodes," *Electrochim. Acta*, **46** [6] 867–74 (2001).

[16]Y. Takeda, Y. Sakaki, H. Y. Tu, M. B. Phillipps, N. Imanishi, and O. Yamamoto, "Perovskite Oxides for the Cathode in Solid-Oxide Fuel Cells," *Electrochemistry*, **68** [10] 764–70 (2000).

[17]A. Mitterdorfer and L. J. Gauckler, "$La_2Zr_2O_7$ Formation and Oxygen Reduction Kinetics of the $La_{0.85}Sr_{0.15}Mn_yO_3$, $O_2(g)$ YSZ system," *Solid State Ionics*, **111** [3–4] 185–218 (1998).

[18]K. Murata and M. Shimotsu, "Yttrium-Substituted (La,Y,Sr)MnO_3 as a SOFC Cathode Material," *J. Ceram. Soc. Jpn.*, **110** [7] 618–21 (2002).

[19]S. Park, J. M. Vohs, and R. J. Gorte, "Direct Oxidation of Hydrocarbons in a Solid-Oxide Fuel Cell," *Nature (London)*, **404** [16] 265–67 (2000).

[20]R. J. Gorte, S. Park, J. M. Vohs, and C. Wang, "Anodes for Direct Oxidation of Dry Hydrocarbons in a Solid-Oxide Fuel Cell," *Adv. Mater.*, **12** [19] 1465–69 (2000).

[21]S. Park, R. Craciun, J. M. Vohs, and R. J. Gorte, "Direct Oxidation of Hydrocarbons in a Solid-Oxide Fuel Cell: I. Methane Oxidation," *J. Electrochem. Soc.*, **146** [10] 3603–605 (1999).

[22]S. Park, R. J. Gorte, and J. M. Vohs, "Tape-Cast Solid-Oxide Fuel Cells for the Direct Oxidation of Hydrocarbons," *J. Electrochem. Soc.*, **148** [5] A443–A447 (2001).

[23]H. Kim, S. D. Park, J. M. Vohs, and R. J. Gorte, "Direct Oxidation of Liquid Fuels in a Solid-Oxide Fuel Cell," *J. Electrochem. Soc.*, **148** [7] A693–A695 (2001).

[24]R. Doshi, C. B. Alcodk, N. Gunasi Karan, and J. J. Carberry, "Carbon Monoxide and Methane Oxidation Properties of Oxide Solid Solution Catalysts," *J. Catal.*, **140** [2] 557–63 (1993).

[25]J. Sfeir, J. Van Herle, and A. J. McEvoy, "Stability of Calcium-Substituted Lanthanum Chromites Used as SOFC Anodes for Methane Oxidation," *J. Eur. Ceram. Soc.*, **19** [6–7] 897–902 (1999).

[26]M. Weston and I. S. Metcafe, "$La_{0.6}Sr_{0.4}Co_{0.2}Fe_{0.8}O_3$ as an Anode for Direct Methane Activation in SOFCs," *Solid State Ionics*, **113–115** [1–4] 247–51 (1998).

[27]J. Liu, B. D. Madsen, Z. Ji, and S. A. Barnett, "A Fuel-Flexible Ceramic-Based Anode for Solid-Oxide Fuel Cells," *Electrochem. Solid-State Lett.*, **5** [6] A122–A124 (2002).

[28]C. W. Tanner, K. Z. Fung, and A. V. Virkar, "The Effect of Porous Composite Electrode Structure on Solid-Oxide Fuel Cell Performance. I. Theoretical Analysis," *J. Electrochem. Soc.*, **144** [1] 21–30 (1997).

[29]K. Kleveland, M.-A. Einarsrud, C. R. Schmidt, S. Shamsili, S. Faalaend, K. Wiik, and T. Grande, "Reactions between Strontium-Substituted Lanthanum Manganite and Yttria-Stabilized Zirconia: II, Diffusion Couples," *J. Am. Ceram. Soc.*, **82** [3] 729–34 (1999).

[30]A. P. Simmer, J. F. Bonnett, N. L. Canfield, K. D. Meinhardt, J. P. Shelton, V. L. Sprenkle, and J. W. Stevenson, "Development of Lanthanum Ferrite SOFC Cathodes," *J. Power Sources*, **113**, 1–10 (2003).

[31]R. Chiba, F. Yoshimura, and Y. Sakurai, "Properties of $La_{1-y}Sr_yNi_{1-x}Fe_xO_3$ as a Cathode Material for a Low-Temperature-Operating SOFC," *Solid State Ionics*, **152–153**, 575–82 (2002).

[32]M. T. Colomer, B. C. H. Steele, and J. A. Kilner, "Structural and Electrochemical Properties of the $Sr_{0.8}Ce_{0.1}Fe_{0.7}Co_{0.3}O_{3-\delta}$ Perovskite as Cathode Material for ITSOFCs," *Solid State Ionics*, **147**, 41–48 (2002).

[33]S. P. Simner, J. F. Bonnett, N. L. Canfield, K. D. Meinhardt, V. L. Sprenkle, and J. W. Stevenson, "Optimized Lanthanum Ferrite-Based Cathodes for Anode-Supported SOFCs," *Electrochem. Solid-State Lett.*, **5** [7] A173–A175, 2002.

[34]A. V. Virkar, J. Chen, C. W. Tanner, and J.-W. Kim, "The Role of Electrode Microstructure on Activation and Concentration Polarizations in Solid-Oxide Fuel Cells," *Solid State Ionics*, **131** [1–2] 189–98 (2000).

[35]H. Kim, C. daRosa, M. Boaro, J. M. Vohs, and R. J. Gorte, "Fabrication of Highly Porous YSZ by Acid Leaching Ni from a Ni-YSZ Cermet," *J. Am. Ceram. Soc.*, **85** [6] 1473–76 (2002).

[36]M. Boaro, J. M. Vohs, and R. J. Gorte, "Synthesis of Highly Porous YSZ by Tape-Casting Methods," *J. Am. Ceram. Soc.*, **86**, 395–400 (2003).

[37]O. A. Marina, N. L. Canfield, and J. W. Stevenson, "Thermal, Electrical, and Electrocatalytical Properties of Lanthanum-Doped Strontium Titanate," *Solid State Ionics*, **149** [1–2] 21–28 (2002). □